Time-Delayed Control of SISO Systems for Improved Stability Margins

A. Galip Ulsoy
ASME Fellow
Department of Mechanical Engineering,
University of Michigan,
Ann Arbor, MI 48109-2125
e-mail: ulsoy@umich.edu

While time delays typically lead to poor control performance, and even instability, previous research shows that time delays can, in some cases, be beneficial. This paper presents a new benefit of time-delayed control (TDC) for single-input single-output (SISO) linear time invariant (LTI) systems: it can be used to improve robustness. Time delays can be used to approximate state derivative feedback (SSD), which together with state feedback (SF) can reduce sensitivity and improve stability margins. Additional sensors are not required since the state derivatives are approximated using available measurements and time delays. A systematic design approach, based on solution of delay differential equations (DDEs) using the Lambert W method, is presented using a scalar example. The method is then applied to both single- and two-degree of freedom (DOF) mechanical systems. The simulation results demonstrate excellent performance with improved stability margins. [DOI: 10.1115/1.4028528]

1 Introduction

Time delays occur in many natural and engineered systems and often lead to problems such as poor control or instability. Linear time delay systems (TDSs) exhibit an infinite number of eigenvalues, which results in difficulties in stability analysis, in obtaining free and forced solutions, as well as controller design [1–4]. However, TDS can also present an opportunity for improved control performance. This paper presents a method that utilizes time delays to approximate SSD, which can be used together with SF to reduce sensitivity and improve stability margins.

1.1 Motivation. Control systems are typically designed based on nominal plant models, and variations in parameters are often encountered in practice. Consequently, recent decades have seen significant research interest in robust control design, where such model uncertainties are explicitly considered in the design process. A variety of methods have been developed for achieving robust control design [5–7]. One of those methods is the use of SSD, in addition to SF, to reduce closed-loop system sensitivity to plant parameter variations and to disturbance inputs [8]. However, SSD is difficult to realize in practice, because additional sensors are needed to measure the state derivatives in addition to the states. Even measuring all the states is too restrictive in many applications; thus, measuring state derivatives as well as states are often impractical. For example, in a single–DOF mechanical system, one would need to measure acceleration, in addition to the states (i.e., position and velocity), to implement SSD feedback. In this paper, the use of time delays in the control to approximate the state derivatives is considered and shown to yield improved stability margins. Consequently, with TDC, the benefits of improved robustness can be realized without the need for additional sensors beyond those required for SF.

1.2 Background. Time delays occur in many engineering systems and can lead to difficulties in controller design and performance. For example, delays can be a significant concern in networked control systems [9,10], in engine control [11,12], or in teleoperation of robots [13]. Such TDS are described by DDEs

and have an infinite eigenspectrum, which makes their analysis and control challenging. Nevertheless, a number of researchers have reported various benefits of using time delays in controller design. For example, Yang and Mote [14,15] have demonstrated that time delays can be used for non-colocated vibration control in bandsawing, to improve accuracy and reduce raw material waste. They use time delays to predict the response of the flexible bandsaw blade structure at points where no sensor is located. Thus, avoiding instability and robustness problems associated with non-colocation of sensors and actuators. Udwadia and co-workers have also shown benefits of TDC for flexible structures [16–18]. They consider large time delays in the controller, comparable to the period of the uncontrolled structure, and demonstrate effective performance for both single– and multi-DOF systems. TDC has also been shown to improve performance for both linear and nonlinear systems with uncertainty [19,20]. The approach uses information in the recent past, through the time delay, to directly estimate the unknown dynamics at any given instant. Delayed resonators utilize delayed position feedback to improve vibration absorber performance [21–23].

Several researchers have recently considered the use of delays to replace derivative feedback [24–26]. Lavaei and co-workers have shown that LTI high-order output feedback controllers can be well-approximated using time delays [27]. Time delays have also been used in a SF controller to approximate integral and derivative actions [28]. Other studies explicitly include delay in the control design, although not necessarily as a derivative approximator [29,30].

The use of SSD, in addition to SF, has previously been shown to reduce closed-loop sensitivity and improve disturbance rejection [8]. However, it requires measurement of state derivatives in addition to the system states, which is often not practical. Consequently, approximate derivatives were considered in Ref. [31]. Those approximations were based on low-pass filters, and it was found that most of the robustness benefits of SSD were then lost. It has also been shown that SSD controllers may be fragile, in the sense that arbitrarily small time delays may destroy stability [32], and that small uncertain feedback delays cannot always be safely neglected if state derivatives are used in the feedback [33]. This occurs when such delays lead to neutral, rather than retarded, DDE's.

In this paper, the approximation of the state derivatives using finite differencing, rather than approximating derivatives via filtering, is considered. This leads to a retarded (not neutral) DDE,

which is then analyzed using a recently developed approach for the analysis and control of TDS based on the Lambert W function [4,34]. Conditions can then be found where the benefits of SSD are achieved with a TDC. To avoid fragility problems associated with SF in the presence of delays, it is important to have such analysis and design tools for appropriate selection of the controller gains and time delay. While other DDE analysis tools (e.g., Ref. [35]) could also be used, the Lambert W approach is quite convenient and efficient.

1.3 Purpose and Scope. The purpose of this paper is to present a new method for improving the robustness (i.e., sensitivity and stability margins) of controlled systems by the intentional use of time delays in the control. In Sec. 2, time delays are used to approximate the derivatives of the state, so that SSD feedback can be approximately achieved without the need for any additional sensors to measure state derivatives. A systematic design approach, based on solution of DDEs via the Lambert W method, and necessary design tools are presented using a scalar example. Sections 3 and 4 present applications of the proposed method to single- and two-DOF mechanical systems, respectively, and present simulation results showing that the desired closed-loop performance can be achieved and with improved stability margins. A summary and conclusions are presented in Sec. 5.

2 Theory With Scalar Example

Consider a SISO LTI plant in state equation form

$$\dot{\mathbf{x}} = \mathbf{A}\mathbf{x} + \mathbf{B}u$$
$$y = \mathbf{C}\mathbf{x} \tag{1}$$

Assuming all states are measurable a SF controller,

$$u(t) = -\mathbf{K}\mathbf{x}(t) \tag{2}$$

yields the closed-loop system equations

$$\dot{\mathbf{x}} = \mathbf{A_c}\mathbf{x} = (\mathbf{A} - \mathbf{B}\mathbf{K})\mathbf{x}$$
$$y = \mathbf{C}\mathbf{x} \tag{3}$$

It is well-known that if $(\mathbf{A}, \mathbf{B})$ is controllable, then $\mathbf{K}$ can be selected (e.g., by eigenvalue assignment or optimal control methods) to achieve the desired closed-loop performance. If not all the states are measured, but $(\mathbf{A}, \mathbf{C})$ is observable, then one can also design a state estimator, or observer, to estimate the states from the output and use those estimated states in the feedback control, e.g., Ref. [36]. Furthermore, the SF controllers can be designed to achieve not only the desired closed-loop performance but can also be designed for excellent robustness properties as measured by stability margins. However, the use of a state estimator will typically reduce those stability margins, e.g., Ref. [37].

2.1 Sensitivity Reduction Via State Derivative Feedback. Consider an SSD feedback controller [8]

$$u(t) = -\mathbf{F}\mathbf{x}(t) - \mathbf{G}\dot{\mathbf{x}}(t) \tag{4}$$

for the system in Eq. (1). The closed-loop system becomes

$$\dot{\mathbf{x}}(t) = \mathbf{A_c}\mathbf{x} = (\mathbf{I} + \mathbf{B}\mathbf{G})^{-1}(\mathbf{A} - \mathbf{B}\mathbf{F})\mathbf{x}(t) \tag{5}$$

As discussed in detail in Ref. [8], one can first select $\mathbf{K}$ in Eq. (2) to obtain a desired $\mathbf{A_c}$ in Eq. (3), then select $\mathbf{G}$ based on sensitivity considerations and to ensure invertability of $(\mathbf{I} + \mathbf{B}\mathbf{G})$, and finally determine $\mathbf{F}$ from Eq. (5) given $\mathbf{A_c}$, $\mathbf{G}$, $\mathbf{A}$, and $\mathbf{B}$.

The use of SSD feedback gives exactly the same closed-loop eigenstructure as SF control, but, for appropriate values of $\mathbf{G}$, can reduce eigenvalue sensitivity to variations in the parameters of $\mathbf{A}$

and $\mathbf{B}$, lead to improved stability margins, and also reduce the effects of any external disturbances acting on the system [8]. Thus, the benefits of SSD feedback over SF control can be significant. For example, it has been shown in Theorem 2 of [8] that the sensitivity of the eigenvalues of the closed-loop matrix $\mathbf{A_c}$ in Eq. (5) can be characterized by

$$S_{\mathbf{A}}^{\lambda_i} = \frac{\partial \lambda_i}{\partial \mathbf{A}} = (\mathbf{I} + \mathbf{B}\mathbf{G})^{-T}\mathbf{y}_i\mathbf{x}_i^T$$
$$S_{\mathbf{B}}^{\lambda_i} = \frac{\partial \lambda_i}{\partial \mathbf{B}} = -(\mathbf{I} + \mathbf{B}\mathbf{G})^{-T}\mathbf{y}_i\mathbf{x}_i^T(\mathbf{F} + \mathbf{G}\mathbf{A_c})^T \tag{6}$$

where λ_i, $i = 1, 2, .~ n$, are the distinct complex eigenvalues of the matrix $\mathbf{A_c}$, the $\mathbf{x}_i$ and $\mathbf{y}_i$ are the corresponding normalized right and left eigenvectors. The state derivative gain, $\mathbf{G}$, can be selected to reduce these sensitivities, then the SF gain, $\mathbf{F}$, can be selected to achieve the desired closed-loop eigenstructure for $\mathbf{A_c}$.

Example 1. Sensitivity reduction by SSD feedback

Let $a = -0.05$ and $b = 1.0$ for the system $\dot{x}(t) = ax(t) + bu(t)$ and consider the SF controller $u(t) = -kx(t)$ to obtain $\dot{x}(t) = a_c x(t) = (a - bk)x(t)$. If one selects, $a_c = -2$, then $k = (a - a_c)/b = 1.95$. Thus, the closed-loop system will have a 2% settling time of $t_s = 4(1/2) = 2$ s, improving on the open-loop settling time of $t_s = 4(20) = 80$ s.

Next, consider the SSD controller $u(t) = -fx(t) - g\dot{x}(t)$ to obtain the closed-loop system $\dot{x}(t) = (1 + bg)^{-1}(a - bf)x(t) = a_c x(t)$. Since $a_c = -2$, for a given g, one can then obtain the required value of f, i.e., $f = (a - a_c(1 + bg))/b$, as summarized in Table 1. Note that, to avoid division by zero, one cannot select $g = -(1/b) = -1$ in this example.

For SSD feedback control, the sensitivity of the closed-loop system eigenvalue (i.e., $\lambda = a_c = -2$) with respect to variations in the open-loop parameters a and b can be obtained as

$$S_a^\lambda = \frac{\partial}{\partial a}[(1 + bg)^{-1}(a - bf)] = (1 + bg)^{-1}$$
$$S_b^\lambda = \frac{\partial}{\partial b}[(1 + bg)^{-1}(a - bf)] = \frac{-(f + ag)}{(1 + bg)^2} \tag{7}$$

For the SF controller, the corresponding sensitivity expressions can be obtained from Eq. (7) when $g = 0$. As shown in Table 1, for $g > 0$, the sensitivities for SSD feedback control (i.e., $g \neq 0$) are reduced compared to SF control (i.e., $g = 0$). The use of SSD feedback also improves the stability margins, as discussed later in this section. Although not shown here, values of $g > 0$ in SSD feedback also reduce the effects of external disturbances acting on the system [8]. Thus, the benefits of SSD feedback can be significant.

2.2 Approximation Via Time Delay. Despite its sensitivity reduction benefits, in practice, it is often difficult to obtain measurements of the state derivatives to implement SSD feedback. As an alternative, the implementation of the following TDC is considered:

$$u(t) = -\mathbf{K_p}\mathbf{x}(t) - \mathbf{K_d}\mathbf{x}(t - h) \tag{8}$$

Table 1 Values of the gain *f*, and sensitivities in Eq. (7), for a given value of the gain *g*, to achieve $a_c = -2$

g	f	S_a^λ	S_b^λ
0	1.95	1	−1.95
1	3.95	0.5	−0.9750
5	11.95	0.1667	−0.3250
10	21.95	0.0909	−0.1773

Note: As g increases the sensitivities are reduced.

where h is a constant time delay. This yields the closed-loop system

$$\dot{\mathbf{x}}(t) = (\mathbf{A} - \mathbf{BK_p})\mathbf{x}(t) - \mathbf{BK_d}\mathbf{x}(t-h) = \mathbf{A_c}\mathbf{x}(t) + \mathbf{A_d}\mathbf{x}(t-h) \tag{9}$$

The system in Eq. (9) is a DDE and has an infinite eigenspectrum. However, in the limit as h approaches zero, Eq. (9) can also be viewed as an approximation to the closed-loop system in Eq. (5) where SSD feedback was utilized. Consider the finite difference approximation, for small h

$$\dot{\mathbf{x}}(t) \approx \frac{\mathbf{x}(t) - \mathbf{x}(t-h)}{h} \tag{10}$$

Then, the SSD feedback control can be approximated as

$$\begin{aligned} u(t) = -\mathbf{Fx}(t) - \mathbf{G}\dot{\mathbf{x}}(t) &\approx -\mathbf{Fx}(t) - (1/h)\mathbf{G}(\mathbf{x}(t) - \mathbf{x}(t-h)) \\ &= -(\mathbf{F} + (1/h)\mathbf{G})\mathbf{x}(t) + (1/h)\mathbf{Gx}(t-h) \end{aligned} \tag{11}$$

Thus, comparing Eqs. (8) and (11), one obtains

$$\begin{aligned} \mathbf{K_p} &= \mathbf{F} + (1/h)\mathbf{G} \\ \mathbf{K_d} &= -(1/h)\mathbf{G} \end{aligned} \tag{12}$$

Consequently, if one selects h to be sufficiently small, and selects $\mathbf{G}$ to reduce sensitivity, the resulting closed-loop system in Eq. (9) will have the specified closed-loop eigenstructure and desired performance (as with SF control only) plus reduced sensitivity, as with SSD feedback control. However, Eq. (9) is a DDE; thus, its analysis, to select the appropriate value of h and to confirm closed-loop performance and robustness, can be challenging.

Example 2. Approximation of state derivative

Consider the scalar system in Ex. 1, and approximate the SSD feedback controller, $u(t) = -fx(t) - g\dot{x}(t)$, by using time delay h in the control, as $u = -k_p x(t) - k_d x(t-h)$. Given f and g, and the time delay h, one can determine the gains k_p and k_d for this controller using Eq. (12). Table 2 summarizes these for $h = 0.1$ s (small relative to the specified closed-loop settling time of 2 s) and selected values of g. Note in Eq. (12) that all elements of $\mathbf{G}$ are divided by h. Thus, the same gains can be obtained by scaling either the time delay or the elements of the gain $\mathbf{G}$. For example, the same gains $k_p = 61.95$ and $k_d = -50$ are obtained for $g = 0.5$ and $h = 0.01$ as for $g = 5$ and $h = 0.1$.

2.3 Solution of Delay Differential Equations. Ideally, one would like to see the performance of the closed-loop system in Eq. (9) be close to that specified by $\mathbf{A_c}$ in Eq. (3) or Eq. (5). The system of DDEs in Eq. (9) possesses an infinite number of eigenvalues due to the presence of the delay h. However, the overall system response, as in higher-order linear systems without delay, will be dominated by the system eigenvalues closest to the imaginary axis; that is the rightmost eigenvalues in the s-plane. These rightmost eigenvalues will determine stability as well as transient response characteristics, such as settling time and overshoot [38]. A method, based on the Lambert W function, has been developed that enables the analysis of LTI TDS as in Eq. (9) to obtain

rightmost eigenvalues and the time response [4]. This method, which will be utilized here to establish the performance of the closed-loop system in Eq. (9), is briefly summarized below.

The solution to an autonomous system of DDEs, $\dot{\mathbf{x}}(t) = \mathbf{A_c}\mathbf{x}(t) + \mathbf{A_d}\mathbf{x}(t-h)$, as in Eq. (9), can be written in terms of an infinite series as [4]

$$\mathbf{x}(t) = \sum_{k=-\infty}^{\infty} e^{\mathbf{S}_k t}\mathbf{C}_k^{\mathbf{I}} \tag{13}$$

where the coefficients $\mathbf{C}_k^{\mathbf{I}}$ depend on a preshape function $\boldsymbol{\phi}(t)$, $-h \leq t < 0$, and

$$\mathbf{S}_k = \frac{1}{h}\mathbf{W}_k(\mathbf{A_d}h\mathbf{Q}_k) + \mathbf{A_c} \tag{14}$$

are the solution matrices, where the matrix $\mathbf{Q}_k$ satisfies

$$\mathbf{W}_k(\mathbf{A_d}h\mathbf{Q}_k)e^{\mathbf{W}_k(\mathbf{A_d}h\mathbf{Q}_k)+\mathbf{A_c}h} = \mathbf{A_d}h \tag{15}$$

An iterative numerical solution of Eq. (15) yields the matrix $\mathbf{Q}_k$, which is then substituted into Eq. (14) to obtain $\mathbf{S}_k$. The rightmost eigenvalues of Eq. (9) can then be obtained from the eigenvalues of $\mathbf{S}_k$, for $k = 0, \pm 1, \ldots, \pm m$, where $m =$ nullity ($\mathbf{A_d}$). The series solution in Eq. (13) converges as k is increased. Software routines available in the LambertW_DDE Toolbox can be utilized to compute both the rightmost eigenvalues and the time response [4,39].

Example 3. Eigenvalues and response of the closed-loop system with TDC

Consider the system in Examples 1 and 2. The closed-loop system is represented by the DDE

$$\begin{aligned} \dot{x}(t) &= (a - bk_p)x(t) - (bk_d)x(t-h) \\ &= -(0.05 + k_p)x(t) - k_d x(t-h) \end{aligned} \tag{16}$$

For different values of g and h, one can obtain the gains k_p and k_d as in Example 2 (see Table 2). Then, for each set of gains, one can determine the rightmost eigenvalue from the analytical expression [4]

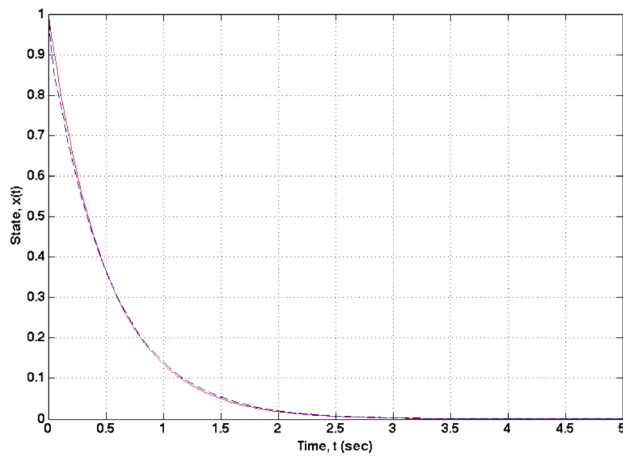$$s_0 = \frac{1}{h}W_0(-bk_d h e^{-(a-bk_p)h}) + (a - bk_p) \tag{17}$$

where W_0 is the principal ($k = 0$) branch of the Lambert W function, W_k. This can be readily evaluated, for example using the lambertw command in MATLAB, or using functions available in the open source LambertW_DDE Toolbox [39]. Other DDE analysis tools, e.g., Ref. [35], could also be utilized. However, only the Lambert W approach is considered here and is found to be very convenient and efficient. These rightmost (i.e., dominant) eigenvalues are given in Table 3 for selected values of g and h. Furthermore, either using the series solution in Eq. (13) or a numerical integration routine (e.g., dde23 in MATLAB), one can obtain the time response for the system in Eq. (16).

The results in Table 3 show that the rightmost eigenvalue is close to the desired value of -2. Given g, as we decrease h, the

Table 2 Values of the gains k_d and k_d in Eq. (12) for given values of g, and for time delay $h = 0.1$ s, to achieve $a_c = -2$

g	f	k_p	k_d
0	1.95	1.95	0
1	3.95	13.95	−10
5	11.95	61.95	−50
10	21.95	121.95	−100

Table 3 Rightmost eigenvalue of Eq. (16) for selected values of g and h

	$h = 0.01$	$h = 0.05$	$h = 0.1$
$g = 0$	−2.0	−2.0	−2.0
$g = 1$	−1.9900	−1.9508	−1.9034
$g = 5$	−1.9835	−1.9206	−1.8484
$g = 10$	−1.9820	−1.9140	−1.8368

Note: As g and h are reduced the rightmost eigenvalue approaches the desired value of -2.0.

Fig. 1 Closed-loop response to initial condition $x(t) = 1.0$ for $-h < t < 0$ for the scalar system in Ex. 3 with SF control (solid red line) and with TDC (dashed blue line) when $g = 1$ and $h = 0.1\,s$
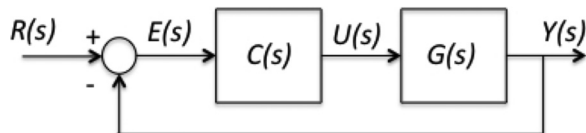
approximation in Eq. (10) becomes more accurate and the closed-loop eigenvalues approach the desired value of -2. As shown in Fig. 1, for $g = 1$ and $h = 0.1\,s$, the time response is very close to the $g = 0$ (i.e., SF only) case with a settling time of approximately 2 s.

In addition to achieving the specified performance, one would like to see improved robustness, for $\mathbf{G} \neq \mathbf{0}$, due to the addition of the time delay terms in the control. Well-known measures of robustness for SISO systems are the stability margins, i.e., gain margin, GM, and phase margin, PM, and these are discussed in Sec. 2.4.

2.4 Stability Margins. Standard measures of the robustness of SISO control systems are their stability margins, i.e., the gain and phase margins. For a typical closed-loop unity feedback system, as in Fig. 2, the stability margins are determined from a Bode (or Nyquist) plot of the loop transfer function $C(s)G(s)$. A typical frequency domain control design rule-of-thumb is to specify $GM > 6\,dB$ and $PM > 30$ to 40 deg. The stability margins can be readily obtained, for example, using the margin command in MATLAB, or simply from a Bode or Nyquist plot of the loop transfer function $C(s)G(s)$ [40]. For a pure time delay of h seconds, the transfer function is $G_D(s) = e^{-sh}$, which in the frequency domain has a constant gain of one (i.e., 0 dB) and a phase of $-\omega h$. For example, when $\omega h = \pi$ rad the delay introduces a phase lag of 180 deg. Consequently, if the desired closed-loop bandwidth is ω_{bw}, then delays of $h \ll \pi/\omega_{bw}$ are desired [40]. The research on stability margins for systems with time delays has been limited [41,42].

Example 4. Stability margins of example system

Consider the system in Examples 1–3. The plant transfer function is $G(s) = b/(s - a) = 1/(s + 0.05)$ and the controller transfer function is $C(s) = k_p + k_d e^{-sh}$. When $h = 0$ (no delay), then $k_d = 0$ and $k_p = k$, for SF control only. The results are summarized in Table 4 for selected values of the SSD feedback gain, g, and the delay time, h, ranging from 5 to 100 ms. As a basis for comparison, when $g = 0$ (SF only) the stability margins are
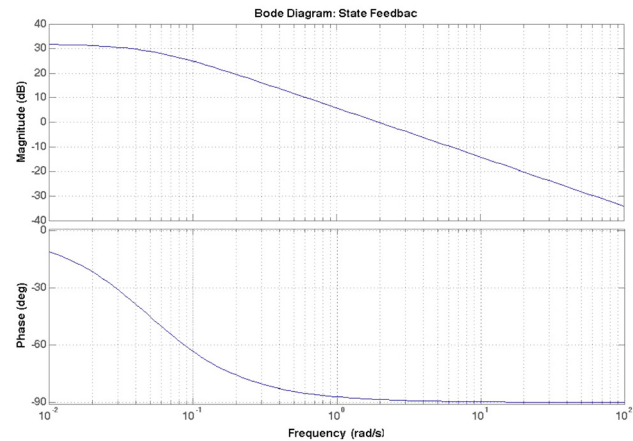

Fig. 2 Block diagram of a SISO unity feedback control system with controller $C(s)$ and plant $G(s)$

Table 4 Phase margins, PM, in degrees, for the closed-loop system in Eq. (16) for combinations of g and h

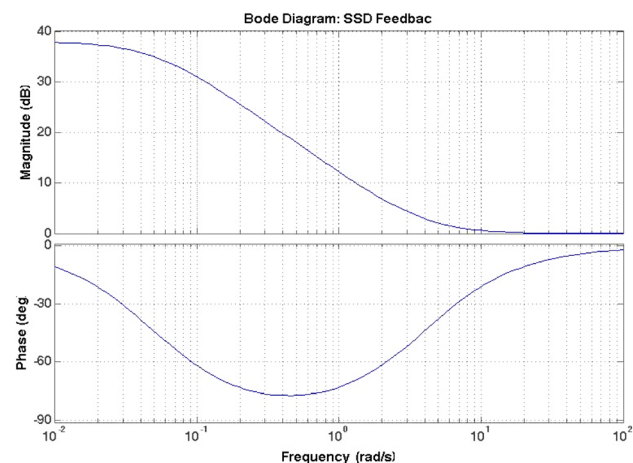|	$h = 0$	$h = 0.005$	$h = 0.01$	$h = 0.05$	$h = 0.1$
$g = 0$	91.5	NA	NA	NA	NA
$g = 0.5$	180	120.8	120.8	120.6	120.0
$g = 0.75$	180	139.1	139.1	138.0	133.5
$g = 1$	180	163.5	156.8	131.1	115.3
$g = 1.25$	180	113.8	112.4	103.3	95.3
$g = 5$	180	31.7	32.1	35.3	39.3
$g = 10$	180	17.6	18.5	26.2	35.7

Note: Note that $g = 0$ is SF only, while $h = 0$ ($g > 0$) is the exact SSD case. With $g > 0$ the SSD case has a PM which is 88.5 deg larger than the SF case. The best PM = 163.5 for $h \neq 0$ is obtained when $g = 1$ and $h = 0.005$.

Fig. 3 Bode plot of $C(s)G(s)$ for SF control. GM $= \infty$ and PM $= 91.5$ deg.

GM $= \infty$ and PM $= 91.5$ deg (see Fig. 3). For exact SSD, without the use of delay to approximate the state derivative, $C(s) = f + gs$ and one obtains GM $= \infty$ and PM $= 180$ deg (see Fig. 4). Consequently, exact SSD, if it were implementable, would nearly double the PM compared to SF control.

Note that when $g > 0$, it is possible to achieve improved phase margins (i.e., greater than 91.5 deg) with the TDC (i.e., approximate SSD using delays). The GM is still infinite, as it was for SF control, and Table 4 shows that phase margins are improved for all values of $g < 1.25$ and $h < 0.1$. For example, when $g = 1$ and

Fig. 4 Bode plot of $C(s)G(s)$ for SSD control with $g = 1$. GM $= \infty$ and PM $= 180$ deg (an improvement in PM of 88.5 deg over SF control)

$h = 0.1$, it is possible to obtain the desired response (see Fig. 1), while improving the phase margin by 23.8 deg (see Fig. 5). When $h = 0.005$ and $g = 1$, the response is indistinguishable from SF control and the phase margin is improved by 72 deg.

For this simple scalar example the frequency response can be analytically obtained for the loop transfer function $H(i\omega) = C(i\omega)G(i\omega)$ as

$$|H(i\omega)| = \sqrt{\text{Re}(H)^2 + \text{Im}(H)^2}$$

$$\angle H(i\omega) = \tan^{-1}\left(\frac{\text{Im}(H)}{\text{Re}(H)}\right)$$

where

$$\text{Re}(H(i\omega)) = -(abk_p + abk_d\cos(\omega h) + bk_d\omega\sin(\omega h))/(\omega^2 + a^2)$$
$$\text{Im}(H(i\omega)) = -(bk_p\omega + bk_d\omega\cos(\omega h) - abk_d\sin(\omega h))/(\omega^2 + a^2)$$

Note that the delay in Eq. (17) leads to transcendental functions in the frequency response, which prevent the gain and phase from becoming small at higher frequencies (see Fig. 3). In general, one can use the Bode or nyquist or margin commands in MATLAB to compute the frequency response numerically. Figures 3–5 show, respectively, the Bode plots for $C(s)G(s)$ for SF control, for SSD feedback with $g = 1$, and TDC (i.e., approximate SSD feedback with $g = 1$ and $h = 0.1$). Note that with SSD feedback, the phase characteristics are improved compared to SF only. Furthermore, the TDC (i.e., approximate SSD) also exhibits improved phase characteristics compared to SF control for frequencies well below $1/h$.

2.5 Comparisons. Consider, for example, a specific numerical comparison to illustrate the benefits of these improved stability margins. Assume the controllers are designed using the given nominal parameter values $a = -0.05$ and $b = 1.0$, but applied to a system with the actual parameter values $a = -0.01$ and $b = 0.5$. Then, the SF controller yields a closed-loop settling time of $t_s = 4.1$ s, the exact SSD controller with $g = 1$ yields $t_s = 3$ s and the approximate SSD controller with $g = 1$ and $h = 0.005$ also yields $t_s = 3$ s. The SSD controllers are less sensitive to the parameter perturbations and lead to settling times closer to the desired value of $t_s = 2$ s. Furthermore, the delay approximation is excellent for this small 5 ms delay time. When the delay time is increased to 100 ms (i.e., $h = 0.1$ s), with $g = 1$, one obtains $t_s = 3.1$ s. Thus, while still a major improvement over the SF case, this approximation with larger delay is slightly less effective compared to the exact SSD controller.
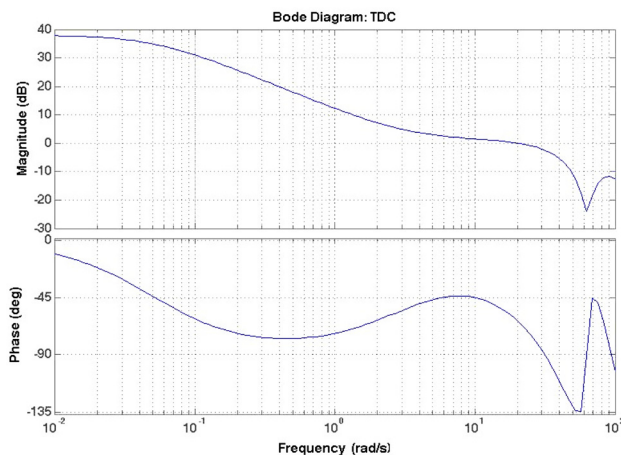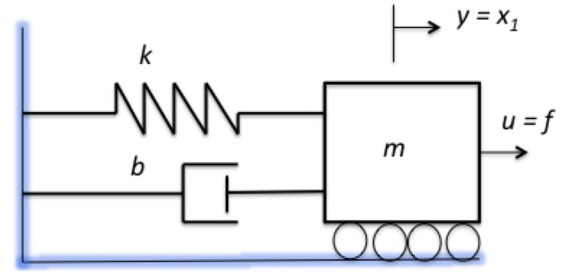

Fig. 6 Schematic of a single-DOF mass-spring-damper system

3 Single–DOF Mechanical Vibration Control

Consider application of the proposed TDC to a single–DOF mechanical system, as in Fig. 6. The system dynamics can be described by the following state equations:

$$\frac{d}{dt}\begin{Bmatrix} x_1 \\ x_2 \end{Bmatrix} = \begin{bmatrix} 0 & 1 \\ -\dfrac{k}{m} & -\dfrac{b}{m} \end{bmatrix}\begin{Bmatrix} x_1 \\ x_2 \end{Bmatrix} + \begin{Bmatrix} 0 \\ \dfrac{1}{m} \end{Bmatrix}u$$

$$y = \begin{bmatrix} 1 & 0 \end{bmatrix}\begin{Bmatrix} x_1 \\ x_2 \end{Bmatrix} \tag{18}$$

and the transfer function of the system is

$$G(s) = \frac{Y(s)}{U(s)} = \frac{(1/m)}{s^2 + (b/m)s + (k/m)} \tag{19}$$

where $x_1 = y$, $x_2 = dy/dt$, and $u = f$. With parameter values $m = k = 1$ and $b = 0.1$, the open-loop system is lightly damped (i.e., open-loop damping ratio $\zeta \approx 0.05$), with a 2% settling time of $t_s \approx 80$ s. The goal is to design a controller to achieve a closed-loop settling time of $t_s \approx 3$ s with little or no overshoot (i.e., closed-loop damping ratio $\zeta \approx 1$).

A SF controller, $u = -\mathbf{K}\mathbf{x} = -K_1 x_1 - K_2 x_2$, requires measurement of position, y, and velocity, $\dot{y}$, and leads to the closed-loop system

$$\frac{d}{dt}\begin{Bmatrix} x_1 \\ x_2 \end{Bmatrix} = \begin{bmatrix} 0 & 1 \\ -\dfrac{(k + K_1)}{m} & -\dfrac{(b + K_2)}{m} \end{bmatrix}\begin{Bmatrix} x_1 \\ x_2 \end{Bmatrix}$$

$$y = \begin{bmatrix} 1 & 0 \end{bmatrix}\begin{Bmatrix} x_1 \\ x_2 \end{Bmatrix} \tag{20}$$

Fig. 5 Bode plot of $C(s)G(s)$ for TDC (i.e., approximate SSD control) with $g = 1$ and $h = 0.1$ s. GM $= \infty$ and PM $= 115.3$ deg (an improvement in PM of 23.8 deg over SF control).
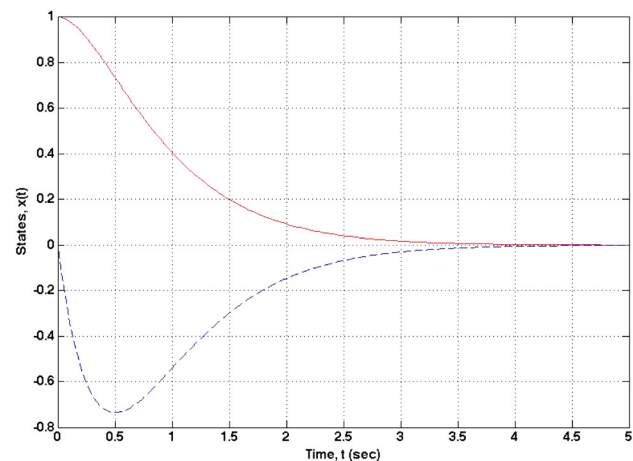

Fig. 7 Response $x(t)$ of single-DOF system with SF control ($K_1 = 3$ and $K_2 = 3.9$) to initial condition $x(0) = [1\ 0]^T$. Red solid line is $x_1(t)$ and dashed blue line is $x_2(t)$.

The controller can also be represented in transfer function form (see Fig. 2) as

$$C(s) = (K_1 + K_2 s) \qquad (21)$$

Selecting desired closed-loop eigenvalues at $s_1 = s_2 = -2$ gives the gains $K_1 = 3$ and $K_2 = 3.9$. The closed-loop response, with $t_s \approx 3$ s and no overshoot as desired, is shown in Fig. 7. The stability margins can be determined from a Bode or Nyquist plot of $C(s)G(s)$, or using the margin command in MATLAB, to be GM $= \infty$ and PM $= 81.1$ deg, so this system also has excellent robustness (see Fig. 8). The closed-loop bandwidth will be $\omega_{\text{bw}} \approx 1$ rad/s. However, the SF controller requires the measurement of velocity, x_2, as well as position, x_1, to implement. Section 4 illustrates how the approximation in Eq. (10) can be used to eliminate the need for velocity measurement, while maintaining the desired closed-loop response and good robustness.

3.1 Approximation of the D term in a Proportional Plus Derivative (PD) controller. As shown in Eq. (21), the SF controller can be viewed as a PD controller, where the derivative of the position (i.e., velocity) is directly measured. As discussed in Ref. [28], a time delay controller can be used to approximate the derivative term, as in Eq. (9). Thus, the TDC becomes

$$u(t) = -K_{\text{p}} x_1(t) - K_{\text{d}} x_1(t - h) \qquad (22)$$

with the controller transfer function

$$C(s) = (K_{\text{p}} + K_{\text{d}} e^{-sh}) \qquad (23)$$

and the closed-loop system is

$$\frac{d}{dt} \begin{Bmatrix} x_1 \\ x_2 \end{Bmatrix} = \begin{bmatrix} 0 & 1 \\ -\dfrac{(k + K_{\text{p}})}{m} & -\dfrac{b}{m} \end{bmatrix} \begin{Bmatrix} x_1(t) \\ x_2(t) \end{Bmatrix}$$
$$+ \begin{bmatrix} 0 & 0 \\ -\dfrac{K_{\text{d}}}{m} & 0 \end{bmatrix} \begin{Bmatrix} x_1(t - h) \\ x_2(t - h) \end{Bmatrix} \quad y = \begin{bmatrix} 1 & 0 \end{bmatrix} \begin{Bmatrix} x_1 \\ x_2 \end{Bmatrix} \qquad (24)$$

Using Eq. (10) to approximate the output derivative term in the PD control gives $K_{\text{p}} = (K_1 + (K_2/h))$ and $K_{\text{d}} = (-K_2/h)$. For example, if one selects $h = 0.1$ then $K_{\text{p}} = 42$ and $K_{\text{d}} = -39$. The response for the system in Eq. (24) is shown in Fig. 9, and can be obtained using routines in the LambertW_DDE Toolbox [39], or the numerical simulation routine dde23 in MATLAB, and is almost
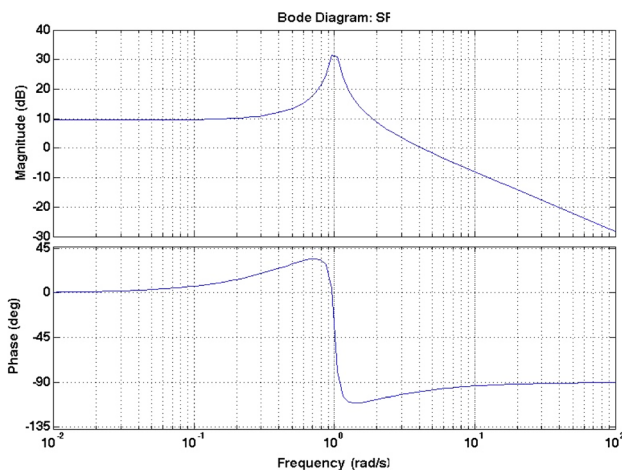

Fig. 9 Response of the single-DOF system with approximate PD control (TDC, $h = 0.1$, $K_{\text{p}} = 42$, and $K_{\text{d}} = -39$) to initial condition $x(0) = [1\ 0]^{\text{T}}$. Red solid line is $x_1(t)$ and dashed blue line is $x_2(t)$.

identical to the response of the system with SF control (see Fig. 7). However, this TDC, which approximates PD control, uses only output (position) measurement.

However, the system with TDC has GM $= 21.7$ dB and PM $= 69.4$ deg when $h = 0.1$ s as shown in the Bode plot in Fig. 10. While these are still excellent stability margins, they do represent a loss of robustness compared to the system with SF. Note that the frequency response plots in Fig. 8 (for SF or PD control) and in Fig. 10 (for TDC, approximate PD control) match very well for frequencies well below $1/h = 10$ Hz $= 20\pi$ rad/s. For smaller values of h that range extends to even higher frequencies. Since the closed-loop system bandwidth is approximately 1 rad/s, this approximation with $h = 0.1$ s is quite effective.

The effect of the time delay, h, on the gains, rightmost poles, and stability margins is summarized in Table 5. Note that as the delay time, h, increases, the rightmost (i.e., dominant) eigenvalue is farther from the desired value of -2, and the stability margins are also reduced. Since typical frequency domain control design guidelines are GM > 6 dB and PM > 30–40 deg, the delays considered here all yield good designs with acceptable closed-loop performance and stability margins. As noted before, when $\omega h = \pi$ rad the delay introduces a phase lag of 180 deg. Consequently, if the desired closed-loop bandwidth is ω_{bw}, then delay times of

Fig. 8 Loop transfer function Bode plot for SF control ($K_1 = 3$ and $K_2 = 3.9$) of single–DOF system. GM $= \infty$ and PM $= 81.1$ deg.
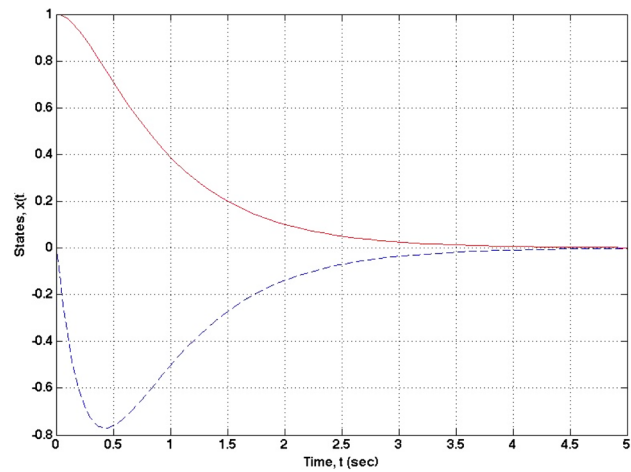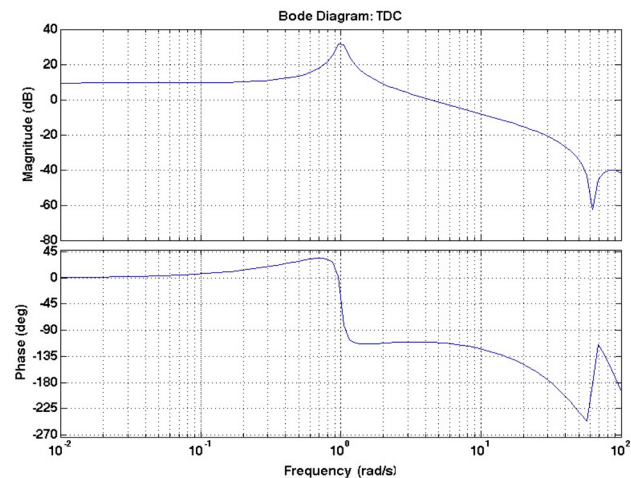

Fig. 10 Loop transfer function Bode plot for approximate PD control (TDC, $h = 0.1$, $K_{\text{p}} = 42$, and $K_{\text{d}} = -39$) of single–DOF system. GM $= 21.7$ dB and PM $= 69.4$ deg.

Table 5 The gains, rightmost poles, and stability margins for the closed-loop system in Eq. (24) with approximate PD control for selected values of the delay time, h

	$h = 0.0001$	$h = 0.0005$	$h = 0.001$	$h = 0.005$	$h = 0.01$	$h = 0.05$	$h = 0.1$
K_p	39003	7803	3903	783	393	81	42
K_d	−39000	−7800	−3900	−780	−390	−78	−39
Rightmost poles	$-2.0 \pm 0.03i$	−1.95 −2.06	$-2.0 \pm 0.06i$	$-2.01 \pm 0.05i$	$-2.01 \pm 0.17i$	$-2.1 \pm 0.30i$	$-2.05 \pm 0.71i$
GM (dB)	82	68.1	62	48.1	42	27.9	21.7
PM (deg)	81	81	80.9	80.5	79.9	75.3	69.4

Note: Note that GM and PM both improve, and the rightmost eigenvalues approach the desired value of −2.0, as $h \rightarrow 0$.

$h \ll \pi / \omega_{\mathrm{bw}}$ are desired. Thus, in this particular example, the closed-loop bandwidth is $\omega_{\mathrm{bw}} \approx 1$ rad/s, and one requires for good performance that $h \ll \pi$. Selecting $h = 0.1$ s, or smaller, is seen to be a good choice from the results in Table 5 for selected values of h.

The rightmost poles in Table 5 are obtained using the Lambert W function method for TDS and the software available in the LambertW_DDE Toolbox [39]. These results illustrate that by using a properly designed TDC, one can measure only position and still achieve performance and stability margins very similar to SF control. Note also that position feedback alone, without delay, simply cannot provide the desired performance (i.e., settling time of 3 s, with no overshoot). In Sec. 4, further robustness improvements are considered by using SSD feedback.

3.2 SSD Control of a Single–DOF Mechanical System.
Consider the SSD feedback control, $u = -\mathbf{Fx} - \mathbf{G\dot{x}} = -F_1 x_1 -F_2 x_2 - G_1 \dot{x}_1 - G_2 \dot{x}_2$, which now requires measurement of position, y, velocity, $\dot{y}$, and acceleration, $\ddot{y}$, of the single-DOF system in Eq. (18). The controller transfer function is

$$C(s) = (F_1 + (F_2 + G_1)s + G_2 s^2) \qquad (25)$$

The closed-loop system can be written as

$$\frac{d}{dt}\begin{Bmatrix} x_1 \\ x_2 \end{Bmatrix} = \begin{bmatrix} 0 & 1 \\ -\dfrac{(k + F_1)}{(m + G_2)} & -\dfrac{(b + F_2 + G_1)}{(m + G_2)} \end{bmatrix} \begin{Bmatrix} x_1 \\ x_2 \end{Bmatrix}$$
$$y = \begin{bmatrix} 1 & 0 \end{bmatrix}\begin{Bmatrix} x_1 \\ x_2 \end{Bmatrix} \qquad (26)$$

to achieve the same closed-loop eigenvalues (i.e., −2 and −2) as with SF, one can select G_1 and G_2, then determine F_1 and F_2 from the equations

$$F_1 = 4(m + G_2) - k; \quad F_2 = 4(m + G_2) - b - G_1 \qquad (27)$$

For example, if one selects $G_1 = 0$, $G_2 = 1.0$, $F_1 = 7$, and $F_2 = 7.9$, the response is exactly the same as in Fig. 7, but with stability margins of GM $= \infty$ and PM = 180 deg (see Fig. 11). So, the system with SSD control has a 98.9 deg increase in the PM compared to SF control only. The disadvantage, of course, is that now one needs to measure not only position and velocity of the mass, but also its acceleration. In Sec. 4, the use of the approximation in Eq. (10) is considered to achieve improved stability margins compared to SF only, but by using only measurement of position and velocity.

3.3 Approximate SSD Control of a Single–DOF Mechanical System. Consider the SSD controller as in Sec. 2, but approximate the state derivative term using Eq. (10). The controller is now given by $u(t) = -\mathbf{K_p x}(t) - \mathbf{K_d x}(t-h) = -K_{p1} x_1(t) - K_{p2} x_2(t) -K_{d1} x_1(t-h) - K_{d2} x_2(t-h)$, which requires only measurement of position, y, and velocity, $\dot{y}$, and has the transfer function

$$C(s) = (K_{p1} + K_{p2}s + K_{d1}e^{-sh} + K_{d2}se^{-sh}) \qquad (28)$$

From Eq. (12), the controller has the gains

$$K_{d1} = -G_1/h; \quad K_{d2} = -G_2/h$$
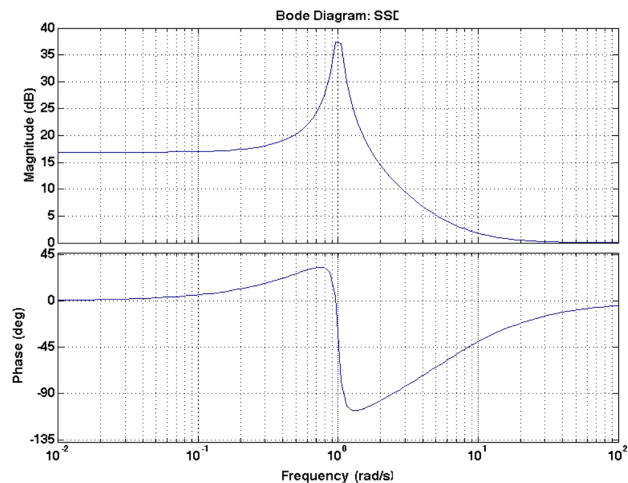$$K_{p1} = F_1 + G_1/h; \quad K_{p2} = F_2 + G_2/h \qquad (29)$$

The closed-loop system is given by

$$\frac{d}{dt}\begin{Bmatrix} x_1 \\ x_2 \end{Bmatrix} = \begin{bmatrix} 0 & 1 \\ -\dfrac{(k + F_1 + G_1/h)}{m} & -\dfrac{(b + F_2 + G_2/h)}{m} \end{bmatrix} \begin{Bmatrix} x_1(t) \\ x_2(t) \end{Bmatrix}$$
$$+ \begin{bmatrix} 0 & 0 \\ \dfrac{G_1}{mh} & \dfrac{G_2}{mh} \end{bmatrix} \begin{Bmatrix} x_1(t-h) \\ x_2(t-h) \end{Bmatrix} \quad y = \begin{bmatrix} 1 & 0 \end{bmatrix}\begin{Bmatrix} x_1 \\ x_2 \end{Bmatrix} \qquad (30)$$

For example, with $G_1 = 0$ and $G_2 = 1.0$ as in Sec. 3.2, one obtains the gains $K_{d1} = 0$, $K_{d2} = -1/h$, $K_{p1} = 7$, and $K_{p2} = 7.9 + 1/h$. Table 6 presents the results for selected values of the delay h.

3.4 Comparisons. The response of the closed-loop system with approximate SSD feedback ($h = 0.1$) is shown in Fig. 12 and is very similar to the response shown in Fig. 7 for the system with SF control. The loop transfer function Bode plot for approximate SSD control ($h = 0.1$) is shown in Fig. 13. For $h = 0.1$ s the PM = 98 deg, which is a 16.9 deg improvement over the SF control. As shown in Table 6, smaller values of h can lead to even larger improvements in the PM. Note that the closed-loop system bandwidth is approximately 1 rad/s, and for frequencies below

Fig. 11 Loop transfer function Bode plot for SSD control ($F_1 = 7$, $F_2 = 7.9$, $G_1 = 0$, and $G_2 = 1$) of a single–DOF system. GM = ∞ and PM = 180 deg.

	$h = 0.005$	$h = 0.01$	$h = 0.05$	$h = 0.1$
Gains	$K_{d1} = 0, K_{d2} = -200,$ $K_{p1} = 7, K_{p2} = 207.9$	$K_{d1} = 0, K_{d2} = -100,$ $K_{p1} = 7, K_{p2} = 107.9$	$K_{d1} = 0, K_{d2} = -20,$ $K_{p1} = 7, K_{p2} = 27.9$	$K_{d1} = 0, K_{d2} = -10,$ $K_{p1} = 7, K_{p2} = 17.9$
Rightmost eigenvalues	$-1.99 \pm 0.10i$	$-1.99 \pm 0.14i$	$-1.93 \pm 0.30i$	$-1.86 \pm 0.41i$
PM (deg)	157	148	115	98

Note: As $h \to 0$, the PM increases and the rightmost eigenvalues approach the desired value of -2.0.

$1/h = 10 \, \text{Hz} = 20\pi$ rad/s, the frequency response curves in Fig. 11 (for SSD control) and in Fig. 13 (for approximate SSD control) match quite well. Consequently, values of $h = 0.1$ s, or smaller, yield good results as shown in Table 6. The gain margins are infinite, as for SF control, and the phase margins are significantly higher than for SF control (e.g., 16.9 deg higher for $h = 0.1$).
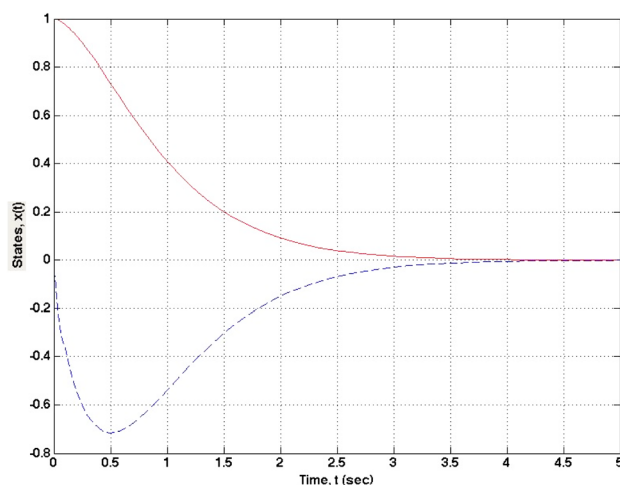
Consequently, the use of time delay for vibration control of the single–DOF mechanical system in Fig. 6 can be beneficial in each of the following ways:

(1) By measuring position only, and using time delay to approximate velocity, one can achieve essentially the same performance as with SF, but with some reduction in stability margins depending on the selected delay time, h.

(2) If both position and velocity are measured to implement SF control, the delay can be used to approximate acceleration and implement approximate SSD feedback, thus, improving stability margins beyond what can be achieved with SF only.
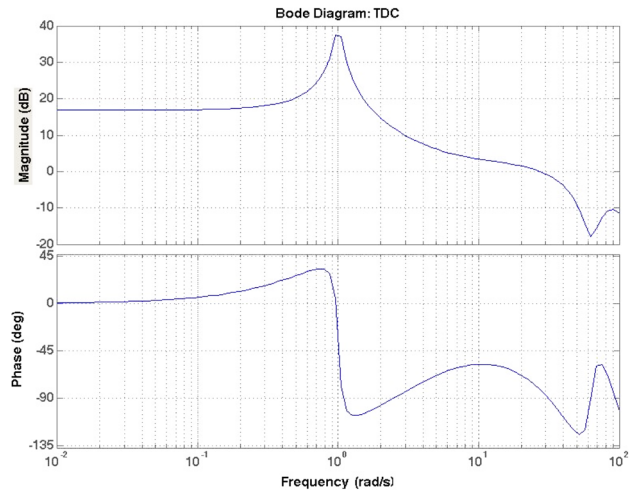
To achieve these robustness benefits of TDC, while maintaining the desired transient response, it is necessary to first design an SSD feedback controller [8], and then select a suitable delay time, h, in approximating the SSD controller using Eq. (10). The recently developed Lambert W function based methods for TDSs, and the open source software LambertW_DDE Toolbox, can be used to facilitate these steps by obtaining rightmost eigenvalues and the time response of the system of DDE's in Eq. (30) [39].

4 Two–DOF Mechanical Vibration Control

Consider next a two–DOF mechanical vibration control problem, similar to the robust control benchmark problem in Ref. [43]. The system is shown in Fig. 14, and the sensor (on mass m_2) and actuator (on mass m_1) are noncolocated. Such noncolocated

Fig. 13 Loop transfer function Bode plot for TDC (approximate SSD control and $h = 0.1$) of a single–DOF system. GM $= \infty$ and PM $= 98$ deg (an improvement in PM of 16.9 deg over SF control).

systems are known to be sensitive to model uncertainty, and have been the subject of numerous robust control studies [43]. The system can be described by the following state equations:

$$\frac{d}{dt}\begin{Bmatrix} x_1 \\ x_2 \\ x_3 \\ x_4 \end{Bmatrix} = \begin{bmatrix} 0 & 0 & 1 & 0 \\ 0 & 0 & 0 & 1 \\ -\left(\frac{k_1 + k_2}{m_1}\right) & \left(\frac{k_2}{m_1}\right) & -\left(\frac{b_1 + b_2}{m_1}\right) & \left(\frac{b_2}{m_1}\right) \\ \left(\frac{k_2}{m_2}\right) & -\left(\frac{k_2}{m_2}\right) & \left(\frac{b_2}{m_2}\right) & -\left(\frac{b_2}{m_2}\right) \end{bmatrix}$$

$$\times \begin{Bmatrix} x_1 \\ x_2 \\ x_3 \\ x_4 \end{Bmatrix} + \begin{Bmatrix} 0 \\ 0 \\ \left(\frac{1}{m_1}\right) \\ 0 \end{Bmatrix} u \quad y = \begin{bmatrix} 0 & 1 & 0 & 0 \end{bmatrix} \begin{Bmatrix} x_1 \\ x_2 \\ x_3 \\ x_4 \end{Bmatrix}$$

$$(31)$$

and the transfer function of the system is given by

Fig. 12 Response of the single–DOF system with TDC (approximate SSD control and $h = 0.1$) to initial condition $x(0) = [1 \ 0]^T$. Red solid line is $x_1(t)$ and dashed blue line is $x_2(t)$.
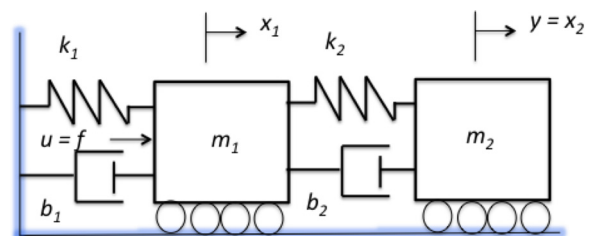

Fig. 14 Schematic of a two–DOF mass–spring–damper system

$$G(s) = \frac{Y(s)}{U(s)} = \frac{(1/m_1)((b_2/m_2)s + (k_2/m_2))}{s^4 + \left(\left(\frac{b_1 + b_2}{m_1}\right) + \left(\frac{b_2}{m_2}\right)\right)s^3 + \left(\left(\frac{k_1 + k_2}{m_1}\right) + \left(\frac{k_2}{m_2}\right) + \left(\frac{b_1 b_2}{m_1 m_2}\right)\right)s^2 + \left(\frac{b_2 k_1 + k_2 b_1}{m_1 m_2}\right)s + \left(\frac{k_1 k_2}{m_1 m_2}\right)} \qquad (32)$$

where $y = x_2$ and $u = f$. With parameter values $m_1 = m_2 = k_1 = k_2 = 1$ and $b_1 = b_2 = 0.1$, the open-loop system response is lightly damped (i.e., open-loop poles at $-0.1309 \pm 1.6127i$ and $-0.0191 \pm 0.6177i$), with a 2% settling time of $t_s \approx 210\,\text{s}$. The goal is to design a controller to achieve a closed-loop settling time of $t_s \approx 4\,\text{s}$ with little or no overshoot (i.e., dominant closed-loop damping ratio $\zeta \approx 1$).

An SF controller, $u = -\mathbf{K}\mathbf{x} = -K_1 x_1 - K_2 x_2 - K_3 x_3 - K_4 x_4$, which requires measurement of the position and velocity or both masses, gives the closed-loop system

$$\frac{d}{dt}\begin{Bmatrix} x_1 \\ x_2 \\ x_3 \\ x_4 \end{Bmatrix} = \begin{bmatrix} 0 & 0 & 1 & 0 \\ 0 & 0 & 0 & 1 \\ -\left(\frac{k_1 + k_2 + K_1}{m_1}\right) & \left(\frac{k_2 - K_2}{m_1}\right) & -\left(\frac{b_1 + b_2 + K_3}{m_1}\right) & \left(\frac{b_2 - K_4}{m_1}\right) \\ \left(\frac{k_2}{m_2}\right) & -\left(\frac{k_2}{m_2}\right) & \left(\frac{b_2}{m_2}\right) & -\left(\frac{b_2}{m_2}\right) \end{bmatrix} \begin{Bmatrix} x_1 \\ x_2 \\ x_3 \\ x_4 \end{Bmatrix}$$

$$y = \begin{bmatrix} 0 & 1 & 0 & 0 \end{bmatrix} \begin{Bmatrix} x_1 \\ x_2 \\ x_3 \\ x_4 \end{Bmatrix} \qquad (33)$$

The controller can also be represented in transfer function form (see Fig. 2) as

$$C(s) = \left(K_1 \left(\frac{s^2 + (b_2/m_2)s + (k_2/m_2)}{(b_2/m_2)s + (k_2/m_2)} \right) + K_2 \right.$$
$$\left. + K_3 s \left(\frac{s^2 + (b_2/m_2)s + (k_2/m_2)}{(b_2/m_2)s + (k_2/m_2)} \right) + K_4 s \right) \qquad (34)$$

Selecting the desired closed-loop eigenvalues at $s_1 = s_2 = -2$, and $s_3 = s_4 = -2.5$, gives the gains $\mathbf{K} = \begin{bmatrix} 23.0 & 1.00 & 8.70 & 33.7 \end{bmatrix}$. The closed-loop response, with $t_s \approx 4\,\text{s}$ and no overshoot as desired, is shown in Fig. 15. The stability margins can be determined from a Bode plot of $C(s)G(s)$ in Fig. 16 to be GM $= \infty$ and

PM $= 71.8$ deg, so this system has the desired performance and excellent robustness characteristics. The SF controller requires measurement of all of the four states (i.e., position and velocity of both masses) to implement.

4.1 SSD Control of a Two–DOF Mechanical System. For the two-DOF system, next consider the SSD feedback control

$$u = -\mathbf{F}\mathbf{x} - \mathbf{G}\dot{\mathbf{x}} = -F_1 x_1 - F_2 x_2 - F_3 x_3 - F_4 x_4 - G_1 \dot{x}_1$$
$$- G_2 \dot{x}_2 - G_3 \dot{x}_3 - G_4 \dot{x}_4 \qquad (35)$$

The controller requires measurement of positions, velocities, and accelerations of both masses and its transfer function is
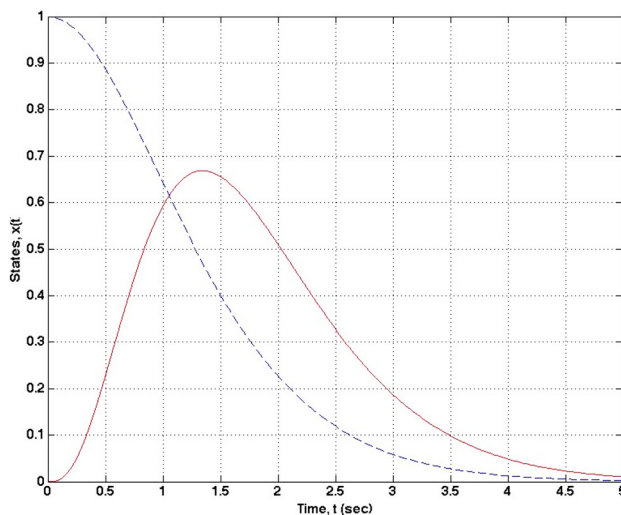

Fig. 15 Response x(t) of two–DOF system with SF control ($K_1 = 23$, $K_2 = 1$, $K_3 = 8.7$, and $K_4 = 33.7$) to initial condition $x(0) = [0\ 1\ 0\ 0]^T$. Solid red line: x_1 and dashed blue line: x_2.

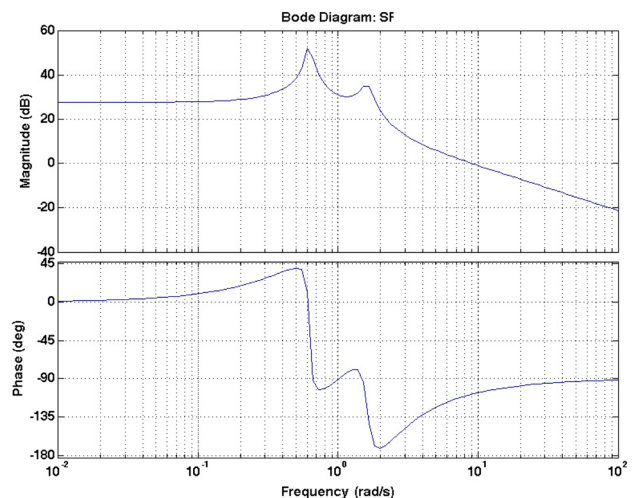Fig. 16 Loop transfer function Bode plot for SF control ($K_1 = 23$, $K_2 = 1$, $K_3 = 8.7$, and $K_4 = 37.7$) of a two–DOF system. GM $= \infty$ and PM $= 71.8$ deg.

$$C(s) = \left(F_1\left(\frac{s^2 + (b_2/m_2)s + (k_2/m_2)}{(b_2/m_2)s + (k_2/m_2)}\right) + F_2\right.$$
$$+ (F_3 + G_1)s\left(\frac{s^2 + (b_2/m_2)s + (k_2/m_2)}{(b_2/m_2)s + (k_2/m_2)}\right) + (F_4 + G_2)s$$
$$\left. + G_3 s^2\left(\frac{s^2 + (b_2/m_2)s + (k_2/m_2)}{(b_2/m_2)s + (k_2/m_2)}\right) + G_4 s^2\right) \qquad (36)$$

The closed-loop system can then be written as

$$\frac{d}{dt}\begin{Bmatrix} x_1 \\ x_2 \\ x_3 \\ x_4 \end{Bmatrix} = \begin{bmatrix} 0 & 0 & 1 & 0 \\ 0 & 0 & 0 & 1 \\ a & b & c & d \\ \left(\dfrac{k_2}{m_2}\right) & -\left(\dfrac{k_2}{m_2}\right) & \left(\dfrac{b_2}{m_2}\right) & -\left(\dfrac{b_2}{m_2}\right) \end{bmatrix}\begin{Bmatrix} x_1 \\ x_2 \\ x_3 \\ x_4 \end{Bmatrix}$$

$$a = -[k_1 + k_2 + F_1 + k_2(G_4/m_2)]/(m_1 + G_3);$$
$$b = [k_2 - F_2 + k_2(G_4/m_2)]/(m_1 + G_3);$$
$$c = -[G_1 + b_1 + b_2 + F_3 + b_2(G_4/m_2)]/(m_1 + G_3);$$
$$d = -[G_2 - b_2 + F_4 - b_2(G_4/m_2)]/(m_1 + G_3);$$

$$y = \begin{bmatrix} 0 & 1 & 0 & 0 \end{bmatrix}\begin{Bmatrix} x_1 \\ x_2 \\ x_3 \\ x_4 \end{Bmatrix} \qquad (37)$$

to achieve the same closed-loop eigenvalues (i.e., -2, -2, -2.5, and -2.5) as with SF, one can select $\mathbf{G}$, then determine $\mathbf{F}$ from the equations
$$F_1 = -a(m_1 + G_3) - k_2(G_4/m_2) - k_1 - k_2$$
$$F_2 = -b(m_1 + G_3) + k_2(G_4/m_2) + k_2$$
$$F_3 = -c(m_1 + G_3) - G_1 - b_2(G_4/m_2) - b_1 - b_2$$
$$F_4 = -d(m_1 + G_3) - G_2 + b_2(G_4/m_2) + b_2 \qquad (38)$$

For example, if one selects $G_1 = G_2 = G_4 = 0$ and $G_3 = 1.0$, Eq. (38) gives $F_1 = 48$, $F_2 = 1$, $F_3 = 17.6$, and $F_4 = 67.3$ to achieve the same closed-loop $\mathbf{A_c}$ as for SF control. One obtains exactly the same response as in Fig. 15, but with stability margins of GM $= \infty$ and PM $= 180$ deg (see Fig. 17). So the system with SSD control has a 108.2 deg increase in the PM compared to SF only. The disadvantage, of course, is that now one needs to measure not only positions and velocities of the two masses, but also their accelerations to implement SSD control. In Sec. 5, the use of the approximation in Eq. (10) is considered to achieve improved stability margins compared to SF only, but using only measurement of positions and velocities.

4.2 Approximate SSD Control of a Two–DOF Mechanical System. Consider the SSD controller in Sec. 3, but approximate the state derivative term using Eq. (10). The controller is given by

$$u(t) = -\mathbf{K_p}\mathbf{x}(t) - \mathbf{K_d}\mathbf{x}(t - h) = -k_{p1}x_1(t) - k_{p2}x_2(t)$$
$$- k_{p3}x_3(t) - k_{p4}x_4(t) - k_{d1}x_1(t - h) - k_{d2}x_2(t - h)$$
$$- k_{d3}x_3(t - h) - k_{d4}x_4(t - h) \qquad (39)$$

This controller requires measurement of only the positions and velocities of the two masses and has the transfer function

$$C(s) = \left[(K_{p1} + K_{d1}e^{-sh})\left(\frac{s^2 + (b_2/m_2)s + (k_2/m_2)}{(b_2/m_2)s + (k_2/m_2)}\right)\right.$$
$$+ (K_{p2} + K_{d2}e^{-sh}) + (K_{p3} + K_{d3}e^{-sh})s$$
$$\left. \times \left(\frac{s^2 + (b_2/m_2)s + (k_2/m_2)}{(b_2/m_2)s + (k_2/m_2)}\right) + (K_{p4} + K_{d4}e^{-sh})s\right] \qquad (40)$$

The closed-loop system is given by

$$\frac{d}{dt}\begin{Bmatrix} x_1(t) \\ x_2(t) \\ x_3(t) \\ x_4(t) \end{Bmatrix} = \mathbf{A_c}\mathbf{x}(t) + \mathbf{A_d}\mathbf{x}(t-h) = \begin{bmatrix} 0 & 0 & 1 & 0 \\ 0 & 0 & 0 & 1 \\ -\left(\dfrac{k_1 + k_2 + K_{p1}}{m_1}\right) & \left(\dfrac{k_2 - K_{p2}}{m_1}\right) & -\left(\dfrac{b_1 + b_2 + K_{p3}}{m_1}\right) & \left(\dfrac{b_2 - K_{p4}}{m_1}\right) \\ \left(\dfrac{k_2}{m_2}\right) & -\left(\dfrac{k_2}{m_2}\right) & \left(\dfrac{b_2}{m_2}\right) & -\left(\dfrac{b_2}{m_2}\right) \end{bmatrix}\begin{Bmatrix} x_1(t) \\ x_2(t) \\ x_3(t) \\ x_4(t) \end{Bmatrix}$$

$$+ \begin{bmatrix} 0 & 0 & 0 & 0 \\ 0 & 0 & 0 & 0 \\ -\left(\dfrac{K_{d1}}{m_1}\right) & -\left(\dfrac{K_{d2}}{m_1}\right) & -\left(\dfrac{K_{d3}}{m_1}\right) & -\left(\dfrac{K_{d4}}{m_1}\right) \\ 0 & 0 & 0 & 0 \end{bmatrix}\begin{Bmatrix} x_1(t-h) \\ x_2(t-h) \\ x_3(t-h) \\ x_4(t-h) \end{Bmatrix} \qquad (41)$$

The controller gains $\mathbf{K_p}$ and $\mathbf{K_d}$ are determined from Eq. (12). For example, using the same SSD gains $\mathbf{F}$ and $\mathbf{G}$ as in Sec. 3, one obtains the gains $K_{d1} = K_{d2} = K_{d4} = 0$, $K_{d3} = -G_3/h = -1/h$, $K_{p1} = F_1$, $K_{p2} = F_2$, $K_{p4} = F_4$, and $K_{p3} = F_3 + G_3/h = F_3 + 1/h$. Table 7 presents the results for selected values of the delay h.

4.3 Comparisons. The closed-loop response of the two DOF system with approximate SSD control is shown in Fig. 18 for $h = 0.1$, and is very similar to the response with SF control (see Fig. 15). The loop transfer function Bode plot for $h = 0.1$ is shown in Fig. 19. Note that for $h = 0.1$ s the PM $= 80$ deg, which is
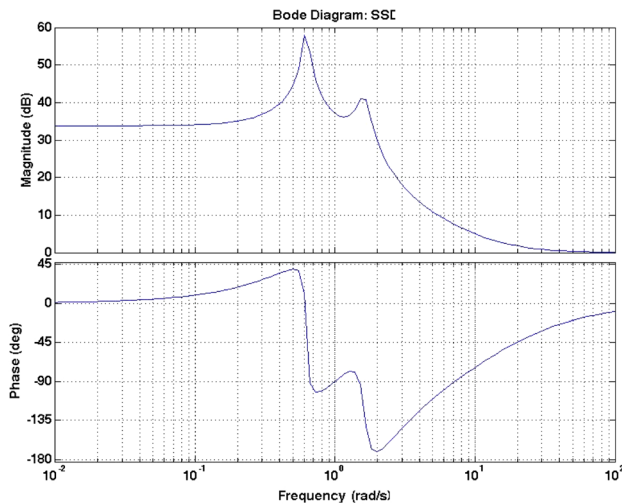
8.2 deg larger than the SF control. This improvement in PM increases as h becomes smaller (see Table 7). Furthermore, the gain margin is infinite as with SF control.

The use of time delay for vibration control of the two DOF mechanical system in Fig. 14, can be beneficial by approximating acceleration to implement approximate SSD feedback, thus, improving stability margins beyond what can be achieved with SF only. To achieve these robustness benefits of time delay control, while maintaining the desired transient response, it is necessary to first design an SSD controller, then approximate it using Eq. (10) as a TDC, then select a suitable delay time, h. These steps can be
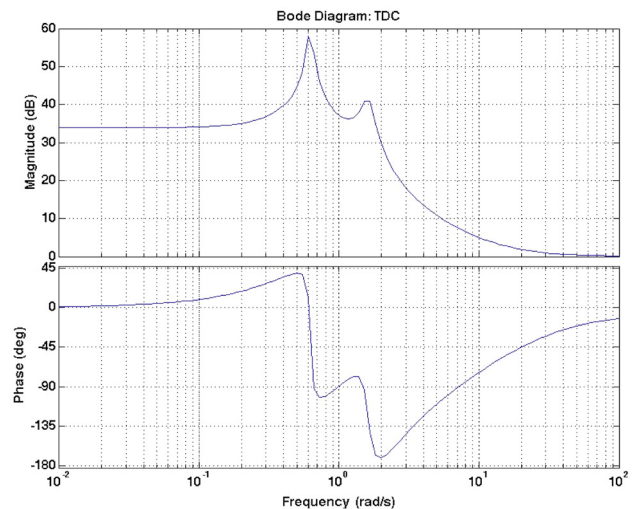
Table 7 Gains, rightmost eigenvalues, and phase margins for the system in Eq. (41) with approximate SSD control with $G_1 = G_2 = G_4 = 0$ and $G_3 = 1.0$ for selected values of h

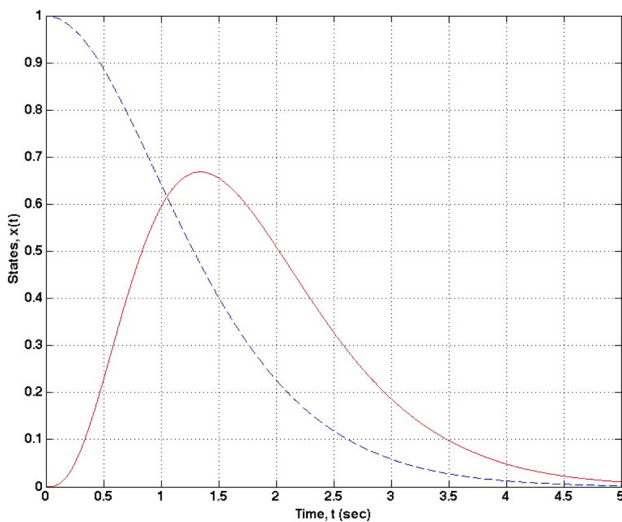|	$h = 0.001$	$h = 0.005$	$h = 0.01$	$h = 0.05$	$h = 0.1$
Gains	$k_{d1} = k_{d2} = k_{d4} = 0$, $k_{d3} = -1000$, $k_{p1} = 48$, $k_{p2} = 1$, $k_{p3} = 1017.6$, $k_{p4} = 67.3$	$k_{d1} = k_{d2} = k_{d4} = 0$, $k_{d3} = -200$, $k_{p1} = 48$, $k_{p2} = 1$, $k_{p3} = 217.6$, $k_{p4} = 67.3$	$k_{d1} = k_{d2} = k_{d4} = 0$, $k_{d3} = -100$, $k_{p1} = 48$, $k_{p2} = 1$, $k_{p3} = 117.6$, $k_{p4} = 67.3$	$k_{d1} = k_{d2} = k_{d4} = 0$, $k_{d3} = -20$, $k_{p1} = 48$, $k_{p2} = 1$. $k_{p3} = 37.6$, $k_{p4} = 67.3$	$k_{d1} = k_{d2} = k_{d4} = 0$, $k_{d3} = -10$; $k_{p1} = 48$, $k_{p2} = 1$, $k_{p3} = 27.6$, $k_{p4} = 67.3$
Rightmost eigenvalues	$-1.92 \pm 0.16i$ $-2.57 \pm 0.30i$	$-1.85 \pm 0.22i$ $-2.62 \pm 0.52i$	$-1.79 \pm 0.26i$ $-2.64 \pm 0.68i$	$-1.63 \pm 0.34i$ $-2.58 \pm 1.20i$	$-1.54 \pm 0.38i$ $-2.43 \pm 1.49i$
PM (deg)	164	146	134	95.1	80

Note: As $h \to 0$, the PM increases and the rightmost eigenvalues approach the desired values of -2.0 and -2.5.

Fig. 17 Loop transfer function Bode plot for SSD control of a two–DOF system. GM $= \infty$ and PM $= 180$ deg (an improvement in PM of 108.2 deg over SF control).

Fig. 19 Loop transfer function Bode plot for TDC (approximate SSD control and $h = 0.1$) of a two–DOF system. GM $= \infty$ and PM $= 80$ deg (an improvement in PM of 8.2 deg over SF control).

Fig. 18 Response $x(t)$ of two–DOF system with approximate SSD feedback ($h = 0.1$) to initial condition $x(0) = [0\ 1\ 0\ 0]^T$. Solid red line: x_1 and dashed blue line: x_2.

facilitated by using the methods for SSD controller design in Ref. [8] as well as the recently developed Lambert W function based methods for TDSs, and the open source software LambertW_DDE Toolbox [39].

5 Summary and Conclusions

This paper has demonstrated that time delays can be used to reduce sensitivity and improve robustness by approximating the state derivatives in a SSD feedback controller. First an ideal SSD controller, assuming measurement of state derivatives, is designed [8]. Then, the state derivatives are approximated using finite differencing and a time delay. Recently developed methods, based on the Lambert W function, for analysis of TDS are used to help select a suitable delay time, h, for a specific SSD gain, **G** [4,39]. The method is demonstrated for SISO vibration control problems, for both single– and two–DOF systems, and shown in simulations to yield the specified performance with improved stability margins when compared to state feedback control only.

In conclusion, TDC can approximate SSD control, and be utilized, without requiring additional measurements, to improve stability margins compared to SF control only. However, the resulting TDS can be challenging to analyze and design. This paper has presented a systematic design approach for such controllers. The approach is based on first designing an SSD feedback controller, and then using a finite difference approximation of the state derivative term using time delays. The appropriate time delay can be selected by solving a system of DDEs, for rightmost eigenvalues and/or time response, using a Lambert W function based method and related open source software.

In this paper, we have considered only SISO LTI systems, and assumed measurement of state variables. The extension of the results presented here to multi-input multioutput LTI systems, and to observer-based controllers, appears to be relatively straightforward but is left to future research. A topic for future research is

the "design problem" where given a desired PM and/or GM one can determine the gains for the TDC and the appropriate delay time h. One could also consider other (e.g., higher-order) approximations in place of Eq. (10). An important remaining topic for future research is, of course, to consider the effects of output measurement noise.

References

[1] Stepan, G., 1989, *Retarded Dynamical Systems: Stability and Characteristic Functions*, Longman Scientific & Technical, Harlow, UK.
[2] Kolmanovskii, V. B., and Myshkis, A., 1999, *Introduction to the Theory and Applications of Functional Differential Equations*, Kluwer Academic Publishers, Dordrecht, The Netherlands.
[3] Niculescu, S. I., and Gu, K., 2004, *Advances in Time-Delay Systems*, Springer Berlin, Heidelberg, Germany.
[4] Yi, S., Nelson, P. W., and Ulsoy, A. G., 2010, *Time Delay Systems: Analysis and Control Using the Lambert W Function*, World Scientific, Singapore.
[5] Doyle, J. C., Glover, K., Khargonekar, P. P., and Francis, B. A., 1989, "State-Space Solutions to Standard H_2 and H_∞ Control Problems," IEEE Trans. Autom. Control, **34**(8), pp. 831–847.
[6] Skogestad, S., and Postlethwaite, I., 2005, *Multivariable Feedback Control–Analysis and Design*, Wiley, Chichester, UK.
[7] Balas, G., Chiang, R., Packard, A., and Safonov, M. G., 2007, *Robust Control Toolbox 3: User's Guide*, Mathworks, Natick, MA.
[8] Haraldsdottir, A., Kabamba, P. T., and Ulsoy, A. G., 1988, "Sensitivity Reduction by State Derivative Feedback," ASME J. Dyn. Syst. Meas. Contr., **110**(1), pp. 84–93.
[9] Lian, F. L., Moyne, J., and Tilbury, D. M., 2002, "Network Design Consideration for Distributed Control Systems," IEEE Trans. Control Syst. Technol., **10**(2), pp. 297–307.
[10] Lian, F. L., Moyne, J., and Tilbury, D. M., 2010, "Modeling and Optimal Controller Design of Networked Control Systems With Multiple Delays," Int. J. Control, **76**(6), pp. 591–606.
[11] Yi, S., Nelson, P. W., and Ulsoy, A. G., 2010, "Design of Observer-Based Feedback Control for Time-Delay Systems With Application to Automotive Powertrain Control," J. Franklin Inst., **347**(1), pp. 358–376.
[12] Ulsoy, A. G., Peng, H., and Çakmakcı, M., 2012, *Automotive Control Systems*, Cambridge University, Cambridge, UK.
[13] Anderson, R. J., and Spong, M. W., 1989, "Bilateral Control Of Teleoperators With Time Delay," IEEE Trans. Autom. Control, **34**(5), pp. 494–501.
[14] Yang, B., and Mote, C. D., Jr., 1990, "Vibration Control of Band Saws: Theory and Experiment," Wood Sci. Technol., **24**(4), pp. 355–373.
[15] Yang, B., and Mote, C. D., Jr., 1992, "On Time Delay in Noncolocated Control of Flexible Mechanical Systems," ASME J. Dyn. Syst. Meas. Contr., **114**(3), pp. 409–415.
[16] Udwadia, F. E., von Bremen, H. F., Kumar, R., and Hosseini, M., 2003, "Time Delayed Control of Structural Systems," Earthquake Eng. Struct. Dyn., **32**(4), pp. 495–535.
[17] Udwadia, F. E., and Phohomsiri, P., 2006, "Active Control of Structures Using Time Delayed Positive Feedback Proportional Control Designs," Struct. Control Health Monit., **13**(1), pp. 536–552.
[18] Udwadia, F. E., von Bremen, H., and Phohomsiri, P., 2007, "Time-Delayed Control Design for Active Control of Structures: Principles and Applications," Struct. Control Health Monit., **14**, pp. 27–61.
[19] Youcef-Toumi, K., and Ito, O., 1990, "A Time Delay Controller for Systems With Unknown Dynamics," ASME J. Dyn. Syst. Meas. Contr., **112**(1), pp. 133–142.
[20] Youcef-Toumi, K., and Reddy, S., 1992, "Analysis of Linear Time Invariant Systems With Time Delay," ASME J. Dyn. Syst. Meas. Contr., **114**(4), pp. 544–555.
[21] Renzulli, M. E., Ghosh-Roy, R., and Olgac, N., 1999, "Robust Control of the Delayed Resonator Vibration Absorber," IEEE Trans. Control Syst. Technol., **7**(6), pp. 683–691.
[22] Elmali, H., Renzulli, M., and Olgac, N., 2000, "Experimental Comparison of Delayed Resonator and PD Controlled Vibration Absorbers Using Electromagnetic Actuators," ASME J. Dyn. Syst. Meas. Control, **122**(3), pp. 514–520.
[23] Hosek, M., and Olgac, N., 2002, "A Single-Step Automatic Tuning Algorithm for the Delayed Resonator Vibration Absorber," IEEE/ASME Trans. Mechatron., **7**(2), pp. 245–255.
[24] Kokame, H., Hirata, K., Konishi, K., and Mori, T., 2001, "Difference Feedback Can Stabilize Uncertain Steady States," IEEE Trans. Autom. Control, **46**(12), pp. 1908–1913.
[25] Villafuerte, R., Mondie, S., and Garrido, R., 2013, "Tuning of Proportional Retarded Controllers: Theory and Experiments," IEEE Trans. Control Syst. Technol., **21**(3), pp. 983–990.
[26] Ramirez, A., Mondie, S., and Garrido, R., 2013, "Proportional Integral Retarded Control of Second Order Linear Systems," Proceedings of the IEEE Conference on Decision and Control, Firenze, Italy, Dec. 10–13, pp. 2239–2244.
[27] Lavaei, J., Sojoudi, S., and Murray, R. M., 2010, "Delay-Based Controller Design for Continuous-Time and Hybrid Applications," http://resolver.caltech.edu/CaltechCDSTR:2010.002
[28] Kwon, W. H., Lee, G. W., and Kim, S. W., 1989, "Delayed State Feedback Controller for the Stabilization of Ordinary Systems," Proceedings of the American Control Conference, Pittsburgh, PA, June 21–23, pp. 292–297.
[29] Diop, S., Kolmanovsky, I., Moraal, P. E., and van Nieuwstadt, M., 2001, "Preserving Stability/Performance When Facing an Unknown Time-Delay," Control Eng. Pract., **9**(12), pp. 1319–1325.
[30] Krstic, M., 2009, *Delay Compensation for Nonlinear, Adaptive and PDE Systems (Systems and Control: Foundations and Applications)*, Birkhauser Science.
[31] Haraldsdottir, A., Kabamba, P. T., and Ulsoy, A. G., 1990, "Control of Linear Systems by Output Proportional Plus Derivative Feedback," ASME J. Dyn. Syst. Meas. Contr., **112**(1), pp. 27–34.
[32] Michiels, W., Vyhlidal, T., Huijberts, H., and Nijmeijer, H., 2009, "Stabilizability and Stability Robustness of State Derivative Feedback Controllers," SIAM J. Control Optim., **47**(6), pp. 3100–3117.
[33] Vyhlidal, T., Michiels, W., Zitek, P., and McGahan, P., 2009, "Stability Impact of Small Delays in Proportional-Derivative State Feedback," Control Eng. Pract., **17**(3), pp. 382–393.
[34] Ulsoy, A. G., 2013, "Improving Stability Margins via Time Delay Control," ASME IDETC, Portland, OR, Aug. 4–7, ASME Paper No. DETC2013-12076.
[35] Breda, D., Maset, S., and Vermiglio, R., 2009, "TRACE-DDE: A Tool for Robust Analysis and Characteristic Equations for Delay Differential Equations," *Topics in Time Delay Systems*, J. J. Loiseau, W. Michiels, S. Niculescu, and R. Sipahi, eds., Springer, pp. 145–155.
[36] Anderson, B. D. O., and Moore, J. B., 1990, *Optimal Control: Linear Quadratic Methods*, Prentice-Hall, Upper Saddle River, NJ.
[37] Safonov, M. G., 1980, *Stability and Robustness of Multivariable Feedback Systems*, MIT, Cambridge, MA.
[38] Yi, S., Nelson, P. W., and Ulsoy, A. G., 2010, "Robust Control and Time-Domain Specifications for Systems of Delay Differential Equations via Eigenvalue Assignment," ASME J. Dyn. Syst. Meas. Control, **132**(3), pp. 031003-1–031003-7.
[39] Yi, S., Duan, S., Nelson, P. W., and Ulsoy, A. G., 2014, "Analysis and Control of Time Delay Systems Using the LambertWDDE Toolbox," *Delay Systems: From Theory to Numerics and Applications* (Advances Delays and Dynamics), T. Vyhlidal, J. F. Lafay, and R. Sipahi, eds., Springer, Heidelberg, Germany, Vol. 1, pp. 271–284.
[40] Franklin, G. F., Powell, J. D., and Emami-Naeini, A., 2010, *Feedback Control of Dynamic Systems*, Pearson Prentice-Hall, Upper Saddle River, NJ.
[41] Bergmans, J. W. M., 2005, "Effect of Loop Delay on Phase Margin of First-Order and Second-Order Control Loops," IEEE Trans. Circuits Syst., **52**(10), pp. 621–625.
[42] Lee, T., Watkins, J. M., and Emami, T., 2007, "A Unified Approach for Stabilization of Arbitrary Order Continuous-Time and Discrete-Time Transfer Functions With Delay," Proceedings of the IEEE Conference on Decision and Control, New Orleans, LA, Dec. 12–14, pp. 2100–2105.
[43] Wie, B., and Bernstein, D. S., 1992, "Benchmark Problem for Robust Control Design (1992 ACC Version)," Proceedings of the American Control Conference, Chicago, IL, June 24–26, pp. 2047–2048.